



Viewpoint set

Refractory high entropy superalloys (RSAs)

Daniel B. Miracle^{a,*}, Ming-Hung Tsai^b, Oleg N. Senkov^{a,c}, Vishal Soni^{d,e},
Rajarshi Banerjee^{d,e}

^a AF Research Laboratory, Materials and Manufacturing Directorate, Wright-Patterson AFB, OH, USA

^b Department of Materials Science and Engineering, National Chung Hsing University, Taichung 402, Taiwan

^c UES, Inc., Dayton, OH, USA

^d Advanced Materials and Manufacturing Processes Institute, University of North Texas, Denton, TX 76207, USA

^e Department of Materials Science and Engineering, University of North Texas, Denton, TX 76207, USA

ARTICLE INFO

Article history:

Received 9 April 2020

Revised 18 June 2020

Accepted 18 June 2020

Keywords:

Metal and alloys

Refractory metals

Superalloy

Mechanical properties

High-temperature deformation

Microstructure

Structural material

ABSTRACT

Complex, concentrated alloys (CCAs) containing refractory principal elements and Al can have microstructures with disordered body-centered cubic (BCC) and ordered B2 phases that are remarkably similar to superalloys. The simple idea of copying superalloy microstructures in these BCC-based refractory alloys introduces a set of audacious challenges. BCC metals and B2 compounds are often brittle at room temperature; the B2 phase is unstable in refractory-Al binaries and reasons for its stability in higher-order systems are a mystery; and many refractory metals and alloys display catastrophic oxidation. Here we discuss opportunities and challenges to develop RSAs as new high temperature structural materials.

Published by Elsevier Ltd on behalf of Acta Materialia Inc.

Introduction

A vast international scientific and engineering effort to exceed the capabilities of nickel-based superalloys has persisted for over six decades. The economic and societal benefits for achieving this goal are immense – increased operating temperatures improve efficiency and reduce emissions in gas turbine engines used for air transport and land-based power generators, each with major economic and environmental impacts. Refractory elements have played a central role in many of the alloy concepts considered, including directionally solidified NiAl eutectic alloys with Cr, Mo, Re, V or W [1–3]; Mo-Nb-Si-B alloys [4,5]; and Ir-Nb-Ta-Ni-Al alloys that were the first to be called refractory superalloys [6,7]. Like conventional superalloys, these latter alloys contained both disordered FCC (A1) and ordered FCC-derivative (L1₂) phases.

Before the FCC-based refractory superalloy publications, an innovative effort was underway to intentionally design BCC-based superalloys [8]. Starting with the B2-ordered NiAl compound, transition metal elements with the disordered BCC (A2) structure were added to produce an A2+B2 microstructural analog to the well-known $\gamma - \gamma'$ superalloy microstructure. By replacing Ni with Ti, a

wide range of ternary and more complex B2-containing alloys were discovered. B2 compounds were established with the constitution X-Al-Y, where X=Ti, Zr and/or Hf and Y=Cr, Mo, Nb, Ta, V and/or W. Alloys with 3 to 6 elements were reported, and some had superalloy-like microstructures consisting of A2+B2 phases. The final publication [9] occurred just two years before the launch of the high-entropy alloy (HEA) field [10,11]. Although the alloys studied by Naka and Khan satisfied subsequent definitions for HEAs and for complex, concentrated alloys (CCAs), their work seems to have been forgotten for nearly two decades.

Refractory high-entropy alloys (RHEAs) and refractory complex, concentrated alloys (RCCAs) were first designed in 2010 [12], six years after the HEA concept was introduced, and intriguing superalloy-like microstructures were discovered in RHEAs four years later [13,14]. Initially thought to contain two A2 phases, three of the reported alloys, AlMo_{0.5}NbTa_{0.5}TiZr, Al_{0.3}NbTaTi_{1.4}Zr_{1.3} and Al_{0.5}NbTa_{0.8}Ti_{1.5}VO_{0.2}Zr, were later shown to have A2+B2 phases, revealing exquisite microstructures of a high volume fraction of nanometer-sized, cuboidal particles that were atomically coherent with the surrounding, thin channels of a matrix phase [15–18]. Since then, other RCCAs have been found with similar microstructures [19,20] and the pioneering work of Naka and Khan work was re-discovered.

* Corresponding author.

E-mail address: daniel.miracle@afresearchlab.com (D.B. Miracle).

This paper (re)introduces refractory superalloys (RSAs) as a broad concept with potential to achieve the long-held goal of significantly surpassing the high temperature structural performance of conventional superalloys. The structural materials community is comfortable with (and a bit in awe of) the $\gamma - \gamma'$ superalloy microstructure, and so it may seem natural to copy this template. However, the challenges provided by RSAs are intimidating and can't be overstated. The B2 phase almost never forms in refractory metal binary alloys with Al, and rules for predicting when the B2 phase forms in ternary and higher-order systems are missing. The reaction pathways responsible for forming the A2+B2 microstructure are unknown, and usually produce an 'inverted' microstructure where the ordered B2 phase is continuous and the A2 phase is discrete. B2 compounds are usually brittle, and most RCCAs have a brittle-to-ductile transition above room temperature. Many refractory metals and alloys suffer from not one, but three different mechanisms of catastrophic environmental degradation that can render them unusable at high temperatures. And essential properties such as creep offer challenges – NiAl is not intrinsically strong in creep [21] and creep hasn't been measured at all in RCCAs. RSAs are a daring, high-risk/high-payoff proposition.

In this paper, the basic features of RSA will be introduced and design principles will be described. Each of the major challenges are discussed more fully, along with concepts that may be explored to address them.

Introducing refractory superalloys (RSAs) – characteristics and challenges

Here we introduce RSAs based on their desired microstructures and elemental make-up. A specific alloy composition can have many microstructures, so we first describe the desired target microstructure. Later, we describe the range of compositions and microstructures actually displayed by RSAs.

A principal feature of an RSA is that it displays an analog to the $\gamma - \gamma'$ microstructure of conventional superalloys. Thus, RSAs should have a high volume fraction of discrete, ordered particles surrounded by thin, continuous channels of a disordered matrix phase. The ordered particles should typically be tens of nanometers, and up to a few hundred nanometers, in size and the disordered channels are usually a few tens of nanometers thick or more. The ordered phase is often cuboidal but may also be spherical. Finally, the ordered and disordered phases are atomically coherent or semi-coherent at their interfaces.

Another defining characteristic is that an RSA contains two or more refractory principal elements. There is no single definition of a refractory metal. Metals with a melting temperature (T_m) above 2200 °C are always included, but metals with T_m as low as 1850 °C are also commonly considered [22]. We use the broader definition, and so Cr, Hf, Ir, Mo, Nb, Os, Re, Rh, Ru, Ta, V, W and Zr are all included. The radioactive element, Tc, is excluded. Although it's not a refractory element, we include Ti as an RSA principal element based on its chemical similarity with other Group 4 elements, its inclusion in Naka and Khan's B2-forming formula, and its common use in RSAs. Al is also included as a principal element in RSAs, since it is commonly used to form the ordered phase. An RSA may have high concentrations of other non-refractory elements, such as Ni or Co, and it may have any number of minority elemental additions.

Of the 13 refractory metals considered here, eight have the BCC structure at T_m , three are HCP (Os, Re, Ru) and two are FCC (Ir and Rh). Thus, an RSA can be based on any of these three crystal structures. FCC-based RSAs offer an improved probability of ductility, while the BCC-based RSAs are likely to be stronger and far more common.

In this paper we focus on BCC-based RSAs, where the ordered phase has the CsCl (B2) structure. The goal is for the disordered A2 phase to be continuous and for the ordered B2 phase to be discrete. However, as noted above, an alloy's microstructure can be manipulated and so for the purpose of this work any alloy that is able to simultaneously display both the A2 and B2 phases is considered an RSA. A disordered BCC phase can be strengthened by a careful distribution of other intermetallic phases, such as σ or Laves, but considerations of coherency are lost. Alternatively, a balance of strength and ductility may be sought by careful microstructural control of two or more intermetallic phases [23]. For example, alloys with the B2 and an orthorhombic (O) phase have been studied in the Al-Nb-Ta-Ti system [24]. These are all important concepts, but they require fundamentally different alloying approaches and design strategies. To maintain focus, these concepts are not included as RSAs and are not discussed in the present paper.

Starting from Naka and Khan [8,9], there are growing reports of A2+B2 RSAs in a range of alloy systems. These constitute a remarkable class of alloys with attractive properties that include modest density and improved strength relative to conventional superalloys. Daunting technical challenges are briefly mentioned in the Introduction. The inverted A2+B2 microstructure must be reversed to obtain the best balance of high temperature strength and room temperature (RT) ductility. The superalloy microstructure seems to result from a spinodal decomposition, raising issues regarding the ability to produce long-term microstructural stability. And in some alloys, the B2 phase becomes unstable at or below expected use temperatures on long-term exposure. These issues are discussed in the following sections, as well as possible approaches and studies to address them.

RSA microstructure, compositions and properties

RCCAs with the best high-temperature strengths usually have single-phase, disordered solid solution microstructures [25,26]. Multi-phase RCCAs are generally stronger than single-phase RCCAs at temperatures below ~800–1000 °C, however they rapidly lose their strength at higher temperatures due to dissolution of secondary phases and relatively low melting temperatures [26]. RCCAs are typically brittle at RT and only a small number of single-phase, disordered solid solution RCCAs are ductile at RT, but they are relatively weak above 1000 °C. One approach to achieve both RT ductility and high temperature strength is to increase the melting temperature and adjust the properties of single-phase, disordered solid solution RCCAs via alloying [25,26]. The carefully designed $\gamma - \gamma'$ microstructure of conventional superalloys is a second approach that is the focus of this viewpoint article. A disordered BCC solid solution matrix phase offers the possibility of RT ductility, and carefully controlling the size, distribution and volume fraction, as well as increasing the solvus temperature, of a stronger, discrete ordered B2 phase improves high-temperature strength. The addition of Al, usually required to form the B2 phase in RSAs, also reduces alloy density and may improve oxidation resistance.

Compositions

The first RSA was reported in the Al-Mo-Nb-Ta-Ti-Zr system as a pseudo-binary between Ta and the AlTi₂Mo B2 phase with partial substitution of Zr for Ti and Nb for Mo [8,9]. An 'inverse' relationship between the ordered and disordered phases was found, and the authors were unsuccessful in reversing these phases. This is the only A2+B2 alloy from Naka and Khan, and the alloy composition was not reported. Nearly 20 years later, a similar microstructure was independently re-discovered using a much different rationale – by applying the high-entropy concept to a palette of refractory and low density elements [14]. Three

Table 1
RCCAs containing a B2 phase.

Alloy (moles)	Alloy (at%)	Phase(s)	Reference(s)
<i>RCCAs containing A2+B2</i>			
AlCrMoTaTi	Al ₂₀ Cr ₂₀ Mo ₂₀ Ta ₂₀ Ti ₂₀	A2+B2+C14+C15+C36	[29]
Al _{0.5} Mo _{0.5} NbTa _{0.5} TiZr	Al _{11.1} Mo _{11.1} Nb _{22.2} Ta _{11.1} Ti _{22.2} Zr _{22.2}	A2+B2+Zr	[19]
AlMo _{0.5} NbTa _{0.5} TiZr	Al ₂₀ Mo ₁₀ Nb ₂₀ Ta ₁₀ Ti ₂₀ Zr ₂₀	A2+B2+Al _x Zr _y	[14–16]
Al _{1.167} NbPd _{0.583} Rh _{0.583}	Al ₃₅ Nb ₃₀ Pd _{17.5} Rh _{17.5}	A2+B2	[56]
Al _{0.25} NbTaTiZr	Al _{5.9} Nb _{23.5} Ta _{23.5} Ti _{23.5} Zr _{23.5}	A2+B2	[19]
Al _{0.3} NbTaTi _{1.4} Zr _{1.3}	Al _{5.7} Nb _{23.5} Ta _{17.6} Ti _{27.2} Zr ₂₆	A2+B2	[14,18]
Al _{0.333} Nb _{0.5} Ta _{0.167} TiZr _{1.333}	Al ₁₀ Nb ₁₅ Ta ₅ Ti ₃₀ Zr ₄₀	A2+B2	[20,34]
Al _{0.5} NbTa _{0.8} Ti _{1.5} V _{0.2} Zr	Al ₁₀ Nb ₂₀ Ta ₁₆ Ti ₃₀ V ₄ Zr ₂₀	A2+B2	[14,17,27,28]
<i>RCCAs containing the B2 phase without A2</i>			
Al _{0.295} Cr _{0.091} Mo _{0.227} NbRe _{0.136} Ti _{0.523}	Al ₁₃ Cr ₄ Mo ₁₀ Nb ₄₄ Re ₆ Ti ₂₃	B2+? ^a	[9]
AlCrMoNbTi	Al ₂₀ Cr ₂₀ Mo ₂₀ Nb ₂₀ Ti ₂₀	B2+Laves	[40]
AlCrMoTaTi	Al ₂₀ Cr ₂₀ Mo ₂₀ Ta ₂₀ Ti ₂₀	B2+Laves	[40]
AlCrMoTi	Al ₂₅ Cr ₂₅ Mo ₂₅ Ti ₂₅	B2+Laves	[40]
Al _{0.33} CrMoTi	Al ₁₀ Cr ₃₀ Mo ₃₀ Ti ₃₀	B2+Laves	[33]
Al _{0.53} CrMoTi	Al ₁₅ Cr _{28.3} Mo _{28.3} Ti _{28.3}	B2+Laves	[33]
AlCr _{0.5} NbTiV	Al _{22.2} Cr _{11.1} Nb _{22.2} Ti _{22.2} V _{22.2}	B2+σ	[31]
AlCrNbTiV	Al ₂₀ Cr ₂₀ Nb ₂₀ Ti ₂₀ V ₂₀	B2+C14+σ	[31]
AlCr _{0.5} Nb _{0.75} TiV _{1.25} Zr _{0.5}	Al ₂₀ Cr ₁₀ Nb ₁₅ Ti ₂₀ V ₂₅ Zr ₁₀	B2+C14+Al ₃ Zr	[32]
Al _{0.167} Fe _{0.167} NbTi _{0.333}	Al ₁₀ Fe ₁₀ Nb ₆₀ Ti ₂₀	B2+? ^a	[9]
AlHfNbTi	Al ₂₅ Hf ₂₅ Nb ₂₅ Ti ₂₅	B2	[41]
Al _{0.167} Hf _{0.333} NbW _{0.167}	Al ₁₀ Hf ₂₀ Nb ₆₀ W ₁₀	B2+? ^a	[9]
AlHfTaTi	Al ₂₅ Hf ₂₅ Ta ₂₅ Ti ₂₅	B2	[41]
Al _{0.429} Mo _{0.095} Nb _{0.286} Ta _{0.095} Ti	Al _{22.5} Mo ₅ Nb ₁₅ Ta ₅ Ti _{52.5}	B2+? ^a	[9]
AlMo _{0.5} NbTa _{0.5} TiZr _{0.5}	AlMo _{0.5} NbTa _{0.5} TiZr _{0.5}	B2+Al _x Zr _y	[19]
Al _{0.356} Mo _{0.096} Nb _{0.471} Ti	Al _{18.5} Mo ₅ Nb _{24.5} Ti ₅₂	B2+? ^a	[9]
Al _{0.495} Mo _{0.202} Nb _{0.323} Ti	Al _{24.5} Mo ₁₀ Nb ₁₆ Ti _{49.5}	B2+? ^a	[9]
Al _{0.5} Mo _{0.5} Nb _{1.33} Ti	Al ₁₅ Mo ₁₅ Nb ₄₀ Ti ₃₀	B2+? ^a	[9]
AlMoNbTi	Al ₂₅ Mo ₂₅ Nb ₂₅ Ti ₂₅	B2	[40]
Al _{0.756} Mo _{1.014} NbTiV _{1.014}	Al _{15.8} Mo _{21.2} Nb _{20.9} Ti _{20.9} V _{21.2}	B2	[57]
Al _{0.472} Mo _{0.075} Nb _{0.264} TiV _{0.075}	Al ₂₅ Mo ₄ Nb ₁₄ Ti ₅₃ V ₄	B2+? ^a	[9]
Al _{0.727} Mo _{0.364} Ta _{0.545} Ti ₂	Al ₂₀ Mo ₁₀ Ta ₁₅ Ti ₅₅	B2+? ^a	[9]
AlMoTaTi ₂	Al ₂₀ Mo ₂₀ Ta ₂₀ Ti ₄₀	B2+? ^a	[9]
AlMoTa _{1.882} Ti ₂	Al ₁₇ Mo ₁₇ Ta ₃₂ Ti ₃₄	B2+? ^a	[9]
Al _{0.667} Mo _{0.17} Ti ₂	Al _{23.5} Mo ₆ Ti _{70.5}	B2+? ^a	[9]
Al _{0.909} Mo _{0.727} Ti ₂	Al ₂₅ Mo ₂₀ Ti ₅₅	B2+? ^a	[9]
AlMoTi ₂	Al ₂₅ Mo ₂₅ Ti ₅₀	B2+? ^a	[9]
Al _{0.431} Nb _{0.392} Ta _{0.137} Ti	Al ₂₂ Nb ₂₀ Ta ₇ Ti ₅₁	B2+O	[24]
AlNbTa _{0.5} TiZr _{0.5}	Al ₂₅ Nb ₂₅ Ta _{12.5} Ti ₂₅ Zr _{12.5}	B2	[19]
Al _{1.167} NbPd _{0.292} Rh _{0.875}	Al ₃₅ Nb ₃₀ Pd _{8.75} Rh _{26.25}	B2+s+unknown	[56]
Al _{1.167} NbPd _{0.583} Ru _{0.583}	Al ₃₅ Nb ₃₀ Pd _{17.5} Ru _{17.5}	B2+σ+unknown	[56]
Al _{0.2} NbTi _{0.13}	Al ₁₅ Nb ₇₅ Ti ₁₀	B2+Nb ₃ Al	[9]
Al _{0.273} NbTi _{0.545}	Al ₁₅ Nb ₅₅ Ti ₃₀	B2+Nb ₃ Al	[9]
Al _{0.857} Nb _{0.714} Ti ₂	Al ₂₄ Nb ₂₀ Ti ₅₄	B2+O, B2+α ₂ , B2+O+α ₂	[58]
AlNbTi ₂	Al ₂₅ Nb ₂₅ Ti ₅₀	B2+? ^a	[9]
Al _{1.14} NbTi _{3.42}	Al _{20.5} Nb ₁₈ Ti _{61.5}	B2+? ^a	[9]
AlNbTiV	Al ₂₅ Nb ₂₅ Ti ₂₅ V ₂₅	B2+σ	[31]
AlNbTiV	Al ₂₅ Nb ₂₅ Ti ₂₅ V ₂₅	B2	[30]
AlNbTiVZr _{0.1}	Al _{24.4} Nb _{24.4} Ti _{24.4} V _{24.4} Zr _{2.4}	B2+Al ₃ Zr ₅	[30]
AlNbTiVZr _{0.25}	Al _{23.5} Nb _{23.5} Ti _{23.5} V _{23.2} Zr _{5.9}	B2+Al ₃ Zr ₅	[30]
AlNbTiVZr _{0.5}	Al _{22.2} Nb _{22.2} Ti _{22.2} V _{22.2} Zr _{11.1}	B2+C14+Al ₃ Zr ₅	[30,31]
AlNbTiVZr	Al ₂₀ Nb ₂₀ Ti ₂₀ V ₂₀ Zr ₂₀	B2+C14+Al ₃ Zr ₅	[30,31]
AlNbTiVZr _{1.5}	Al _{18.2} Nb _{18.2} Ti _{18.2} V _{18.2} Zr _{27.3}	B2+C14+Al ₃ Zr ₅	[30]
Al _{0.273} NbZr _{0.545}	Al ₁₅ Nb ₅₅ Zr ₃₀	B2+? ^a	[9]
Al _{0.586} Ta _{0.862} Ti ₂	Al ₁₇ Ta ₂₅ Ti ₅₈	B2+? ^a	[9]
AlTaTi ₂	Al ₂₅ Ta ₂₅ Ti ₅₀	B2+? ^a	[9]
Al _{0.407} TiV _{0.22}	Al ₂₅ Ti _{61.5} V _{13.5}	B2+? ^a	[9]

^a The B2 phase is confirmed in this alloy, but the presence and identification of other phases is not reported.

alloys in this recent work (AlMo_{0.5}NbTa_{0.5}TiZr, Al_{0.3}NbTaTi_{1.4}Zr_{1.3}, Al_{0.5}NbTa_{0.8}Ti_{1.5}V_{0.2}Zr) showed a nano-scale, basket-weave structure in SEM images characteristic of RSA microstructures. All of these have since been confirmed to show the inverted A2+B2 RSA microstructure [15–18,27,28]. Since [14], many more RCCAs have been found with the B2 compound (Table 1, alloys are sorted alphabetically and by concentration, and alloy families are separated by horizontal lines). Sixteen elements (Al–Cr–Fe–Hf–Mo–Nb–Pd–Re–Rh–Ru–Si–Ta–Ti–V–W–Zr) have been used. All alloys in Table 1 have Al and all but five have Ti. Other commonly used elements include Nb (40 alloys), Mo (23 alloys), Ta (16 alloys) and Zr (15 alloys). W, Re and Ru each occur in only one alloy, Rh is found in two alloys and three alloys use Pd. An A2+B2 microstructure is found in

eight distinct alloys drawn from five different alloy families. All but two of these alloys have Al–Nb–Ta–Ti–Zr. Forty-seven alloys, representing 25 different alloy families, show the B2 compound without an A2 phase. These alloys are either a single-phase B2 or they include other intermetallic phases such as σ, Laves (C14), or the orthorhombic O phase based on Ti₂AlNb. This represents a rich opportunity for the exploration of new RSAs that may provide a balance of high-temperature strength and RT ductility.

Microstructures

A typical A2+B2 (or β – β′) RSA microstructure is shown in Fig. 1 [28]. The similarity to Ni-based superalloy microstructures

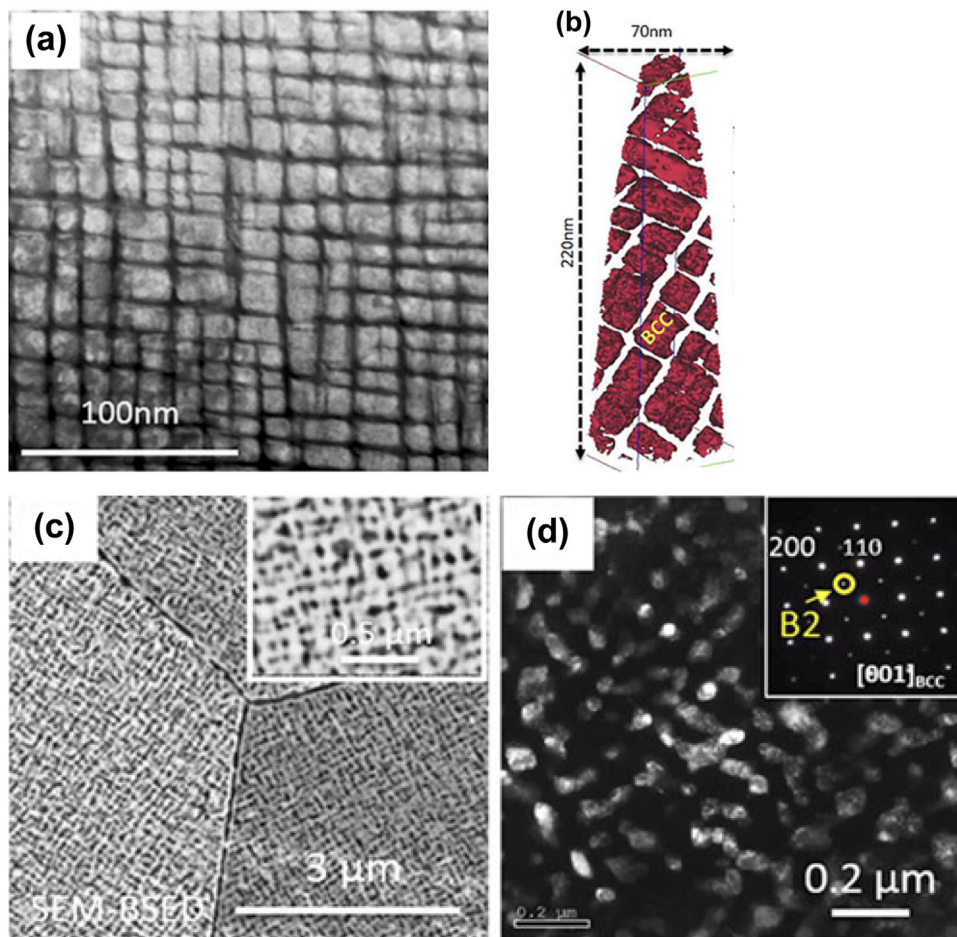


Fig. 1. (a,b) A characteristic RSA microstructure for $\text{Al}_{0.5}\text{NbTa}_{0.8}\text{Ti}_{1.5}\text{V}_{0.2}\text{Zr}$ (atom percent $\text{Al}_{10}\text{Nb}_{20}\text{Ta}_{16}\text{Ti}_{30}\text{V}_4\text{Zr}_{20}$) after annealing at 1200 °C for 24 h and furnace cooling at 10 °C/min to RT. The discrete phases are a disordered BCC (A2) solid solution, and the continuous channels have the CsCl (B2) ordered crystal structure. (c,d) The same material after inverting the continuous and discontinuous phases by annealing at 600 °C for 120 h and water quenching. The images are reproduced from [28] with permissions.

is striking. The extremely fine $\beta - \beta'$ microstructure can appear as a nano-lamellar, basket-weave structure in SEM images and the B2 superlattice peaks are often missing in X-ray diffraction, and so TEM is usually required to characterize these alloys and identify ordering [19]. The discrete phase can be cuboidal or spherical, and needle-like B2 morphologies have been observed [19]. The ordered and disordered phases in Fig. 1a, b are inverted from a typical $\gamma - \gamma'$ microstructure, but a simple thermal treatment gives the normal relationship between the phases (Fig. 1c, d) [17,27,28]. High temperature deformation can also reverse the phases to produce a 'normal' RSA microstructure [19]. The ability to 'flip' this inverted structure by thermal treatment has been observed in at least one other alloy, and the proposed mechanism for producing the desired microstructure – a combination of coarsening and modulus mismatch between the A2 and B2 phases – gives some hope that this process may be universal [18]. Nevertheless, more work is needed to demonstrate generality of this approach.

In addition to the A2+B2 constituents, other phases may occur. An ordered hexagonal phase rich in Al and Zr is found at grain boundaries in $\text{AlMo}_{0.5}\text{NbTa}_{0.5}\text{TiZr}$ [15,19]. Three Laves phases (C14, C15 and C36) occur in AlCrMoTaTi [29], and at least one of these is at grain boundaries. An omega phase (ω) with hexagonal symmetry is seen in $\text{Al}_{0.5}\text{NbTa}_{0.8}\text{Ti}_{1.5}\text{V}_{0.2}\text{Zr}$, and an ordered omega phase (ω^*) is found in the same alloy after annealing at 600 °C, both of these phases are rich in Ti and Zr [28].

Mechanical properties

RSAs and B2-containing RCCAs studied in the as-cast and/or annealed conditions have RT compressive yield strengths ranging from 1000 to 2200 MPa [14,16,19,20,30–34]. Compressive yield strengths drop substantially to 200 – 935 MPa at 1000 °C and to 50–250 MPa at 1200 °C. All but two show limited compressive ductility (<10%) at RT, and so are probably brittle in tension. All reported RSAs show extensive compressive ductility at 1000 °C and above. At intermediate temperatures, RSAs show a mixture of strong/brittle and weak/ductile properties. $\text{AlNbTiVZr}_{0.5}$ [30] and $\text{Al}_{10}\text{Nb}_{15}\text{Ta}_5\text{Ti}_{30}\text{Zr}_{40}$ [20,34] appear to be ductile at RT. A low degree of long-range chemical ordering (LRO) is claimed to be responsible for ductility in $\text{AlNbTiVZr}_{0.5}$. In addition, this alloy also has a much smaller grain size than more Zr-lean alloys in the study, and it has a much lower volume fraction of Laves and Al_3Zr_5 phases relative to more Zr-rich alloys [33]. Further, the compression samples have an initial aspect ratio of 1.5:1, and an aspect ratio of 1:1 is produced in constant volume samples after a uniform compressive strain of only 24%. The stress-strain curve shows a distinct change after about 15% strain and the sample goes well beyond 24% strain, so the degree of unconstrained compressive plastic deformation is uncertain. High RT compressive ductility (above 50%) in $\text{Al}_{10}\text{Nb}_{15}\text{Ta}_5\text{Ti}_{30}\text{Zr}_{40}$ was explained by the presence of a nanometer-level co-continuous mixture of A2 and B2 phases and a low APB energy in the B2 phase [34].

The objective proposed here is to develop RSAs to extend the maximum use temperature of conventional superalloys by 200 °C. As a benchmark, the MAR-M247® blade alloy has a tensile yield strength of about 380 MPa at a maximum use temperature near 1000 °C [35] and so RSAs must provide this same strength at 1200 °C while maintaining all other MAR-M247® properties. Strength – temperature goals can similarly be set to exceed disk or sheet superalloys, where exemplars are INCONEL® 718 and Haynes® 230®, respectively. The design of RSA microstructures follows the superalloy template – a weak, ductile matrix provides plasticity, and well-dispersed, nanometer-sized hard intermetallic particles give strength at elevated temperature [26]. Single-phase, solid solution RCCAs begin to lose strength rapidly above about 65% of the absolute melting temperature, (T_m) [26], while superalloys maintain useful strengths up to 75% of T_m . In both cases the maximum use temperature increases with increasing T_m . The goal of RSA microstructural design is to similarly extend useful strengths beyond what is typical in single-phase RCCAs while also providing RT tensile ductility and damage tolerance.

The balance of properties that may be possible in RSAs are by no means bounded by the current RSA properties described above. Mechanical properties are exceptionally sensitive to composition and microstructure and RSA compositions and microstructures have not yet been optimized. For example, most current RSAs are likely to have a continuous B2 matrix, reducing RT ductility. Inverting this ‘backward’ microstructure significantly increases RT compressive ductility while retaining a yield strength of over 1300 MPa from RT to 600 °C [17]. Good strength and ductility may be possible even with a continuous B2 phase – $\text{Al}_{10}\text{Nb}_{15}\text{Ta}_5\text{Ti}_{30}\text{Zr}_{40}$ has a co-continuous A2+B2 microstructure with good RT compressive strength and ductility [20]. Another feature that unnecessarily restricts current RSA properties is that the B2 phase in some RSAs dissolves above 600 °C [28], limiting reported elevated temperature strengths. Optimizing RSA microstructures requires knowledge of phase equilibria, reaction pathways and constituent properties of the A2 and B2 phases. Challenges associated with these goals are discussed in the remainder of this paper.

Creep properties are almost absent from the RCCA literature. Once alloys with sufficiently stable A2+B2 microstructures are produced, creep properties need to be considered.

Environmental resistance

Conventional refractory metals and alloys generally suffer from rapid oxidation, but attack rates can be up to two orders of magnitude lower in RCCAs [25,36]. The most oxidation resistant RCCAs have high levels of Al, Cr and/or Si and are brittle, but may be considered as coatings for RSA base alloys with better mechanical properties. Studies of composition effects on oxidation mechanisms and kinetics are moving ahead briskly, but there is almost no work on the rate of interstitial element penetration and the influence on phase stability and mechanical properties. Interstitial elements typically embrittle refractory metals, but the strength and ductility are both increased significantly in HfNbTiZr with intentional additions of up to 2% O [37]. Clearly, much more work is needed to explore the generality of this effect.

Phase equilibria

Phase diagrams – the alloy designers’ atlas

Phase diagrams are essential for designing microstructure. We seek phase diagrams that possess an A2+B2 two-phase field with particular reactions that can control the size, volume fraction and distribution of these phases. A ‘sloping solvus’ reaction controls

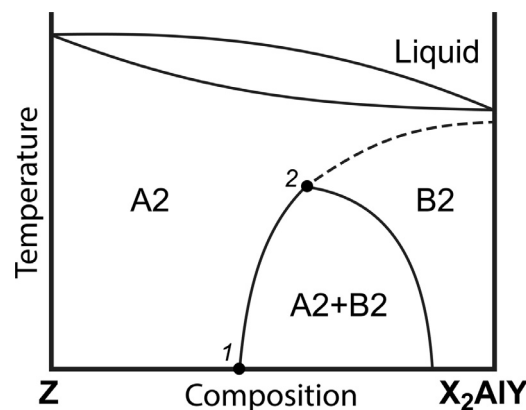


Fig. 2. A pseudo-binary schematic phase diagram between element Z and compound X_2AlY , illustrating a spinodal decomposition from the A2 (to the left of point 2) or the B2 (to the right of point 2) phase field. The dashed line shows a second-order phase transformation representing ordering of the A2 phase upon decreasing temperature at a fixed composition or upon increasing the X_2AlY concentration at a fixed temperature. Redrawn from [9].

microstructures in age-hardened aluminum, conventional superalloys and $\alpha+\beta$ titanium alloys. In these reactions, a two-phase alloy is heated above the use temperature to partially or fully dissolve one of the phases, it's then quenched to retain a supersaturated solid solution, and it's finally aged at an intermediate temperature to control the distribution of the second phase. This simple reaction is attractive for RSAs, and efforts to find phase diagrams with this reaction are needed.

A second common approach for controlling two-phase microstructures is through eutectic or eutectoid reactions. By far the most common commercial example is steels and cast irons, which use the Fe-C eutectoid and eutectic reactions, respectively. Eutectic reactions have also been considered for earlier high temperature alloy concepts such as NiAl eutectics [1–3] and the Mo-Nb-Si-B family of alloys [4,5]. An eutectoid reaction involving the ternary B2 phase in the Al-Nb-Ti phase diagram has been suggested, but this reaction is not likely to involve the disordered A2 phase [38].

A spinodal reaction may produce inverted RSA microstructures in some RCCAs [9,16,20,27]. Naka and Khan used a schematic, pseudo-binary phase diagram to explain the origin of the inverted microstructure (Fig. 2). They proposed that the boundary between points 1 and 2 was nearly vertical for their Ta – $(\text{Ti,Zr})_2\text{Al}(\text{Mo,Nb})$ alloys, so that essentially all compositions within the A2+B2 phase field transformed from the A2 to the B2 phase as they cooled continuously from the solidus temperature, and then finally precipitated discrete A2 particles in the continuous B2 parent phase. However, if this schematic diagram is correct, it may be possible to *quench* from the A2 phase field directly into the A2+B2 field, bypassing the B2 phase and producing the desired RSA microstructure. Such experiments are suggested in future studies.

In other phase diagrams, the B2 phase may form solely by an order-disorder reaction from the parent A2 phase. This second-order phase transformation doesn't produce a two-phase A2+B2 phase field. Alloys that demonstrate this reaction pathway are not useful for RSAs.

Experimental and computational phase diagrams – a missing link

The alloy designer's first step is to scan published phase diagrams, and knowing the desired phase fields and reactions significantly narrows the search. Binary phase diagrams are a poor guide for RSAs, since only one (Al-Mo) of the 15 binary systems drawn from the Al-Mo-Nb-Ta-Ti-Zr family reports a B2 phase, and a recent assessment assigns an A2 structure to the AlMo phase [39]. Rela-

tively few relevant ternary phase diagrams are available and they offer only incomplete data, so that phase fields and reaction pathways can often only be inferred. And essentially no experimental phase diagrams are available for quaternary and higher order systems. Clearly, experimental phase diagram studies are desperately needed.

Phase diagram calculations often fill the experimental gap, but RSAs once again offer unique challenges. The B2 phase rarely occurs in binary phase diagrams with a refractory metal, so CALPHAD PHase Diagram (CALPHAD) databases generally omit this phase from the list of thermodynamic models. At least one RCCA study shows agreement between observation of the B2 phase with CALPHAD calculations [40], but the vast majority of studies show that CALPHAD predicts an A2 phase instead of the B2 phase in RCCAs [20,26,31,32,41].

RSAs also challenge *ab initio* methods. High-throughput density functional methods can determine the lowest energy phase for a given alloy by calculating the total energy for all conceivable competing phases. This has become a tractable problem for binary alloys at well-defined compositions that correspond to stoichiometric compounds. However, RCCAs generally have more principal elements than compounds have sublattices, and calculating the total energy for every possible configuration becomes an insurmountable task. Further, it's difficult to achieve chemical equilibrium between two or more phases in *ab initio* calculations due to the extremely limited simulation timescales. New approaches, such as the multi-cell Monte Carlo ((MC)²) method [42], are just now coming online to address these issues, but much work is yet needed before techniques like this are ready to search the vast RSA composition space. *ab initio* methods may also provide help by performing calculations on ternary systems that can refine CALPHAD databases.

Fundamentals for B2 stability

In the absence of phase diagrams, establishing the fundamental principles that underlie phase stability may give useful insights. Structure maps have been built by considering atomic properties that may influence the structural stability of compounds [43]. These properties include atomic size, electronegativity and valence. Such methods have been applied to binary, pseudo-binary and selected ternary compounds [44]. Extending these concepts may guide efforts to design RSAs with a B2 phase.

The B2 phase appears in selected RCCAs even though it's absent in the constituent binary systems and so it's fair to ask, "does entropy play a role in stabilizing the complex B2 phase"? With only two sublattices but three or more principal elements (Table 1), some degree of chemical mixing must occur on one or both sublattices in complex B2 phases [45]. Here we calculate the configurational entropy of a ternary B2 phase in an Al-Nb-Ti alloy using the sublattice model [46], which is essentially a weighted Boltzmann equation on the different sublattices. The inputs include the number of sites per unit cell for each sublattice and the atomic concentrations on each sublattice. The Al, Nb and Ti concentrations on the two sublattices of the B2 structure were determined [47] using the Atom Location by Channeling Enhanced Microanalysis (ALCHEMI) technique [48]. The configurational entropy of this Al-Nb-Ti B2 phase is thus calculated to be $S = 0.61R$. This is much larger than the configurational entropy of a perfectly ordered, binary B2 structure ($S = 0$), and it is two-thirds the value of a disordered A2 alloy with the same composition. B2 phases with more than three principal elements may have even higher configurational entropies.

At 900 K, this configurational entropy lowers the Gibbs energy relative to a perfectly ordered B2 phase by about 4.5 kJ/mol, and it's tempting to conclude that this reduced energy stabilizes the ternary B2 compound. However, the intermetallic phases that out-

compete the B2 phase in binary systems may also have higher configurational entropies in multi-component systems. The B2 phase may gain more entropy than competing intermetallic phases if it's less choosy about what elements occupy each sublattice. Compounds that are relatively intolerant of atomic substitutions due to requirements of atomic size, valence, electronegativity or bond hybridization may thus become less favored in RCCAs.

In this way, compounds may be entropy-stabilized in RCCAs, and these effects can occur to different degrees in different compounds. Understanding the fundamentals of how compound stabilities are influenced in alloys where there are more principal elements than the compounds have sublattices is a major focus for future research.

Deformation of complex, refractory B2 phases

The B2 structure occurs in a very wide range of alloy systems, and it displays an equally wide range of defect structures, deformation modes and properties [49]. Nevertheless, as a broad generalization, B2 compounds are brittle. The issue is that the preferred $a<100>$ Burgers vector gives only 3 independent strains. $a<111>$ dislocations operate at RT in a small number of B2 compounds (CuZn and FeAl are the best known), offering the potential for ductility. The slip vector can be changed by alloying – Cr, Mn or Fe additions to NiAl successfully changed the slip mode from $a<100>$ to $a<111>$ [50,51]. An entire class of B2 compounds were recently found to be ductile [52], and some contain RSA principal elements Ti or Zr [53]. These compounds initially deform via $a<100>$ slip but transition to $a<110>$ and $a<111>$ after some amount of plastic deformation [53]. This mechanism may explain the large RT compressive ductility of AlNbTiVZr_{0.5} [30]. A low anti-phase boundary (APB) energy and deformation via pairs of $a/2<111>$ screw dislocations are the features of a ductile Al₁₀Nb₁₅Ta₅Ti₃₀Zr₄₀ alloy [34]. Finally, elastic and plastic constraints at boundaries or interfaces may locally produce $a<110>$ or $a<111>$ dislocations, where they're needed most for strain compatibility [54]. So while B2 compounds are typically brittle, RSAs offer scope for ductility through alloying and via constraints at the coherent A2/B2 interfaces.

Summary and a challenge

In this viewpoint article we develop ideas supporting the exploration of refractory superalloys (RSAs) as structural materials that may significantly exceed the use temperature of conventional nickel-based superalloys. This is a long-held goal with immense societal impact, but new capabilities are needed: better control over the brittle-to-ductile transition temperature in BCC alloys; significantly improved oxidation resistance of refractory alloys; and clear principles to guide the development of refractory alloys containing a stable B2 phase at high temperatures. Some of these are enduring challenges that remain unsolved after many decades, but the concentrated solid solutions offered by RCCAs and RSAs offer new approaches. We define RSAs to include FCC-, HCP- and BCC-based alloys, and we focus here on BCC-based microstructures consisting of a disordered A2 matrix with a high volume fraction of atomically coherent, nanometer-sized B2 particles. Much work is already underway, this article formalizes the field, defines distinct challenges blocking progress and offers thoughts to guide the next steps.

Exploration

We challenge the community to expand the range of studied RSA compositions. Current compositions explore variations on the first reported A2+B2 alloys in the Al-Mo-Nb-Ta-Ti-Zr system. Several elements identified by Naka and Khan remain under-represented in

RSAs, and the alloys in Table 1 also include elements not considered by Naka and Khan. Especially, Pd, Pt and Ru all form a stable B2 phase with Al. AlRu melts congruently at 2060 °C and forms an eutectic reaction with Ru at 1920 °C [55]. Following the initial concept by Naka and Khan, AlRu may be alloyed with BCC refractory metals in search of an A2+B2 microstructure. Also, Al may not be absolutely required, and the B2 phase is found in some binary refractory metal systems such as Nb-Ru and Ru-Zr. Finally, the ability to control microstructure should be specifically considered in selecting new alloys for exploration. The search for reaction pathways capable of producing RSA microstructures is suggested, including sloping solvus and eutectic reactions, as well as quenching to form 'normal' RSA microstructure in spinodal systems.

Phase equilibria

A desperate need exists for high quality phase diagrams in ternary and higher order refractory metal systems, including Al. Many decades ago, phase diagram studies were considered important contributions to basic science, but they seem to have fallen out of favor by research proposers and funding agencies alike. This trend needs to be reversed. Experimental phase diagrams are an essential starting point to guide compositional studies and to build thermodynamic models of ternary and higher order B2 phases. Standard approaches in carefully selected systems as well as high-throughput methods including diffusion multiples can make rapid contributions. And new approaches for calculating phase equilibria in complex, concentrated alloys need to be developed and employed.

Fundamentals of compound stability

RSAs offer many unanswered fundamental questions. What stabilizes the B2 phase in ternary and higher order alloys? Do elements have specific site occupancy preferences, and what drives them? Are some atoms ambivalent to which sublattice is occupied? What roles do atom size, valence, electronegativity and bond hybridization play in compound stability? Is configurational entropy important? Since phase equilibrium is a competition, this information is also needed for other intermetallic phases.

Determining site occupancies is fundamental to compound stability, but it is a challenging experimental problem in ternary systems and is essentially insurmountable in more complex alloys using conventional techniques. Computations may play an important role in exploring these questions, and new experimental methods may become available.

Deformation studies and mechanical properties

Although B2 compounds are typically brittle, they can show ductility when $a\langle 110 \rangle$ or $a\langle 111 \rangle$ dislocations operate. *The deformation modes that operate in complex, refractory B2 compounds need to be established.* If only $a\langle 100 \rangle$ dislocations operate, the conditions necessary to activate non- $a\langle 100 \rangle$ dislocations need to be established. Approaches to alter the slip vector can include alloying, decreasing the level of ordering, reducing APB energy or decreasing the size of B2 precipitates. Studying intrinsically ductile B2 compounds and the role of elastic and plastic constraints at interfaces in the RSA microstructures may also provide new insights.

Above all, the most compelling imperative is to determine if a balance of both RT ductility and exceptional high temperature strength can be achieved through the engineered contributions of the A2 and B2 phases in RSA microstructures.

Declaration of Competing Interest

The authors declare that they have no known competing financial interests or personal relationships that could have appeared to influence the work reported in this paper.

Acknowledgments

DBM wishes to acknowledge the AF Research Laboratory, Materials and Manufacturing Directorate, for support to conduct this study. MHT is was supported by the Ministry of Science and Technology, Taiwan (under grant MOST 108-2218-E-005-003) and the "High Entropy Materials Center" from The Featured Areas Research Center Program within the framework of the Higher Education Sprout Project by the Ministry of Education (MOE) and from the Project MOST 109-2634-F-007-024 by Ministry of Science and Technology (MOST) in Taiwan. Work by ONS was supported through the Air Force on-site contract FA8650-15-D-5230 managed by UES, Inc., Dayton, OH, USA. VS and RB have been supported by the U.S. Air Force Office of Scientific Research under contract FA9550-17-1-0395 for work conducted at the University of North Texas.

References

- [1] J.L. Walter, H.E. Cline, *Metall. Trans.* 1 (1970) 1221–1229.
- [2] R.D. Noebe, F.J. Ritzert, A. Misra, R. Gibala, in: *Prospects For Ductility and Toughness Enhancement of NiAl By Ductile Phase Reinforcement*, NASA Technical Memorandum 103796, 1991, p. 20.
- [3] H. Bei, G.M. Pharr, E.P. George, *J. Mater. Sci.* 39 (2004) 3975–3984.
- [4] J.H. Schneibel, C.T. Liu, D.S. Easton, C.A. Carmichael, *Mater. Sci. Eng. A* A261 (1–2) (1999) 78–83.
- [5] R. Sakidja, J.H. Perepezko, *Metall. Mater. Trans. A* 36A (2005) 507–514.
- [6] X. Yu, Y. Yamabe-Mitarai, Y. Ro, Y. Gu, H. Harada, *Scr. Mater.* 41 (6) (1999) 651–657.
- [7] X.H. Yu, Y. Yamabe-Mitarai, Y. Ro, H. Harada, *Metall. Mater. Trans. A* 31 (1) (2000) 173–178.
- [8] S. Naka, T. Khan, *J. Phase Equilib.* 18 (6) (1997) 635–649.
- [9] S. Naka, T. Khan, J.H. Westbrook, R.L. Fleischer (Eds.), *John Wiley & Sons Ltd*, New York, NY, 2002.
- [10] B. Cantor, I.T.H. Chang, P. Knight, A.J.B. Vincent, *Mater. Sci. Eng. A* 375–377 (2004) 213–218.
- [11] J.-W. Yeh, S.-K. Chen, S.-J. Lin, J.-Y. Gan, T.-S. Chin, T.-T. Shun, C.-H. Tsau, S.-Y. Chang, *Adv. Eng. Mater.* 6 (5) (2004) 299–303.
- [12] O.N. Senkov, G.B. Wilks, D.B. Miracle, C.P. Chuang, P.K. Liaw, *Intermetallics* 18 (2010) 1758–1765.
- [13] O.N. Senkov, S.V. Senkova, C. Woodward, *Acta Mater.* 68 (2014) 214–228.
- [14] O.N. Senkov, C. Woodward, D.B. Miracle, *JOM* 66 (10) (2014) 2030–2042.
- [15] J.K. Jensen, B.A. Welk, R.E.A. Williams, J.M. Sosa, D.E. Huber, O.N. Senkov, G.B. Viswanathan, H.L. Fraser, *Scr. Mater.* 121 (2016) 1–4.
- [16] O.N. Senkov, D. Isheim, D.N. Seidman, A.L. Pilchak, *Entropy* 18 (102) (2016) 1–13.
- [17] V. Soni, O.N. Senkov, B. Gwalani, D.B. Miracle, R. Banerjee, *Sci. Rep.* 8 (8816) (2018) 1–10.
- [18] V. Soni, *Phase Transformations in Refractory High Entropy Alloys*, Materials Science and Engineering, University of North Texas, Denton, TX USA, 2019.
- [19] O.N. Senkov, J.K. Jensen, A.L. Pilchak, D.B. Miracle, H.L. Fraser, *Mater. Des.* 139 (2018) 498–511.
- [20] V. Soni, O.N. Senkov, J.-P. Couzinie, Y. Zheng, B. Gwalani, R. Banerjee, *Materialia* 9 (2020) 100569.
- [21] D.B. Miracle, *Acta Metall. Mater* 41 (3) (1993) 649–684.
- [22] Wikipedia, *Refractory metals*, 2020. https://en.wikipedia.org/wiki/Refractory_metals. (Accessed 13 Mar 2020).
- [23] C. Tiwary, V.V. Gunjal, D. Banerjee, K. Chattopadhyaya, *MATEC Web of Conferences* 14 (2014) 01005 1–6.
- [24] J. Peng, S. Li, Y. Mao, X. Sun, *Mater. Lett.* 53 (1–2) (2002) 57–62.
- [25] O.N. Senkov, D.B. Miracle, K. Chaput, J.-P. Couzinie, *J. Mater. Res.* 33 (19) (2018) 3092–3128.
- [26] O.N. Senkov, S. Gorrse, D.B. Miracle, *Acta Mater.* 175 (2019) 394–405.
- [27] V. Soni, B. Gwalani, T. Alam, S. Dasari, Y. Zheng, O.N. Senkov, D. Miracle, R. Banerjee, *Acta Mater.* 185 (2020) 89–97.
- [28] V. Soni, B. Gwalani, O.N. Senkov, B. Viswanathan, T. Alam, D.B. Miracle, R. Banerjee, *J. Mater. Res.* 33 (19) (2018) 3235–3246.
- [29] B. Gorr, F. Mueller, H.J. Christ, H. Chen, A. Kauffmann, R. Schweiger, D.V. Szabó, M. Heilmair, in: *Proceedings of the TMS 147th Annual Meeting & Exhibition, Supplemental Proceedings*, TMS, 2018, pp. 647–659.
- [30] N.Y. Yurchenko, N.D. Stepanov, S.V. Zhurebtsov, M.A. Tikhonovsky, G.A. Salishchev, *Mater. Sci. Eng. A* 704 (2017) 82–90.

- [31] N.Y. Yurchenko, N.D. Stepanov, A.O. Gridneva, M.V. Mishunin, G.A. Salishchev, S.V. Zharebtsov, J. Alloys Compd. 757 (2018) 403–414.
- [32] N. Yurchenko, E. Panina, M. Tikhonovsky, G. Salishchev, S. Zharebtsov, N. Stepanov, Mater. Lett. (2020) 264.
- [33] S. Laube, H. Chen, A. Kauffmann, S. Schellert, F. Müller, B. Gorr, J. Müller, B. Butz, H.J. Christ, M. Heilmaier, J. Alloys Compd. (2020) 823.
- [34] O.N. Senkov, J.-P. Couzinie, S.I. Rao, V. Soni, R. Banerjee, Materialia 9 (2020) 1–16 100627.
- [35] M. Kaufman, in: M. Gell (Ed.), Proceedings of the Fifth International Symposium on Superalloys, Metallurgical Society of AIME, Warrendale, PA, 1984, pp. 43–52.
- [36] T.M. Butler, High Entropy Alloys: Oxidation, Encyclopedia of Metals and Alloys, Elsevier, Submitted.
- [37] Z. Lei, X. Liu, Y. Wu, H. Wang, S. Jiang, S. Wang, X. Hui, Y. Wu, B. Gault, P. Kontis, D. Raabe, L. Gu, Q. Zhang, H. Chen, H. Wang, J. Liu, K. An, Q. Zeng, T.-G. Nieh, Z. Lu, Nature 563 (22 Nov) (2018) 546–552.
- [38] A. Hellwig, M. Palm, G. Inden, Intermetallics 6 (2) (1998) 79–94.
- [39] D.M. Cupid, O. Fabrichnaya, F. Ebrahimi, H.J. Seifert, Intermetallics 18 (6) (2010) 1185–1196.
- [40] H. Chen, A. Kauffmann, S. Seils, T. Boll, C.H. Liebscher, I. Harding, K.S. Kumar, D.V. Szabó, S. Schlabach, S. Kauffmann-Weiss, F. Müller, B. Gorr, H.J. Christ, M. Heilmaier, Acta Mater. 176 (2019) 123–133.
- [41] F.G. Coury, T. Butler, K. Chaput, A. Saville, J. Copley, J. Foltz, P. Mason, K. Clarke, M. Kaufman, A. Clarke, Mater. Des. 155 (2018) 244–256.
- [42] C. Niu, W. Windl, M. Ghazisaeidi, Scr. Mater. 132 (2017) 9–12.
- [43] D.G. Pettifor, Solid State Commun. 51 (1) (1984) 31–34.
- [44] D.G. Pettifor, Mater. Sci. Technol. 4 (8) (1988) 675–691.
- [45] D.B. Miracle, O.N. Senkov, Acta Mater. 122 (2017) 448–511.
- [46] M. Hillert, Phase Equilibria, Phase Diagrams and Phase Transformations: Their Thermodynamic Basis, 2nd ed., Cambridge University Press, Cambridge, UK, 2008.
- [47] D. Banerjee, T.K. Nandy, A.K. Gogia, Scr. Metall. 21 (1987) 597–600.
- [48] J.C.H. Spence, J. Taftø, J. Microsc. 130 (2) (1983) 147–154.
- [49] I. Baker, Mat. Sci. Eng. A A192/193 (1995) 1–13.
- [50] D.B. Miracle, S. Russell, C.C. Law, in: C.T. Liu, A.I. Taub, N.S. Stoloff, C.C. Koch (Eds.), High-Temperature Ordered Intermetallic Alloys III, Materials Research Society Symposium Proceedings, Pittsburgh, PA, 1989, pp. 225–230.
- [51] D.K. Patrick, K.-M. Chang, D.B. Miracle, H.A. Lipsitt, in: L.A. Johnson, D.P. Pope, J.O. Stiegler (Eds.), High-Temperature Ordered Intermetallic Alloys IV, Materials Research Society Symposium Proceedings, Pittsburgh, PA, 1991, pp. 267–272.
- [52] K. Gschneidner, A. Russell, A. Pecharsky, J. Morris, Z. Zhang, T. Lograsso, D. Hsu, C.H. Chester Lo, Y. Ye, A. Slager, D. Kesse, Nat. Mater. 2 (9) (2003) 587–591.
- [53] S.R. Agnew, T. Ungar, IOP Conf. Ser. Mater. Sci. Eng. 580 (2019) 012001.
- [54] D.B. Miracle, Acta Metall. Mater. 39 (7) (1991) 1457–1468.
- [55] S.N. Prins, L.A. Cornish, W.E. Stumpf, B. Sundman, Calphad 27 (1) (2003) 79–90.
- [56] P. Cerba, M. Vilasi, B. Malaman, J. Steinmetz, J. Alloys Compd. 201 (1) (1993) 57–60.
- [57] A. Lacour-Gogny-Goubert, Z. Zhao-Huvelin, A. Bachelier-Locq, I. Guilot, A. Denquin, Mater. Sci. Forum 941 (2018) 1111–1116.
- [58] P.K. Sagar, D. Banerjee, K. Muraleedharan, Y.V.R.K. Prasak, Metall. Mater. Trans. A 27A (1996) 2593–2604.